Available online at www.sciencedirect.com
SCIENCE DIRECT®
Journal of Applied Geophysics 55 (2004) 77–90
JOURNAL OF APPLIED GEOPHYSICS
www.elsevier.com/locate/jappgeo

New method for quantification of vuggy porosity from digital optical borehole images as applied to the karstic Pleistocene limestone of the Biscayne aquifer, southeastern Florida

Kevin J. Cunningham[a,*], Janine I. Carlson[b], Neil F. Hurley[b]

[a] U.S. Geological Survey, 9100 NW 36th Street, Suite 107, Miami, FL 33178, USA
[b] Department of Geology and Geological Engineering, Colorado School of Mines, 1516 Illinois Street, Golden, CO 80401, USA

Abstract

Vuggy porosity is gas- or fluid-filled openings in rock matrix that are large enough to be seen with the unaided eye. Well-connected vugs can form major conduits for flow of ground water, especially in carbonate rocks. This paper presents a new method for quantification of vuggy porosity calculated from digital borehole images collected from 47 test coreholes that penetrate the karstic Pleistocene limestone of the Biscayne aquifer, southeastern Florida. Basically, the method interprets vugs and background based on the grayscale color of each in digital borehole images and calculates a percentage of vuggy porosity. Development of the method was complicated because environmental conditions created an uneven grayscale contrast in the borehole images that makes it difficult to distinguish vugs from background. The irregular contrast was produced by unbalanced illumination of the borehole wall, which was a result of eccentering of the borehole-image logging tool. Experimentation showed that a simple, single grayscale threshold would not realistically differentiate between the grayscale contrast of vugs and background. Therefore, an equation was developed for an effective subtraction of the changing grayscale contrast, due to uneven illumination, to produce a grayscale threshold that successfully identifies vugs. In the equation, a moving average calculated around the circumference of the borehole and expressed as the background grayscale intensity is defined as a baseline from which to identify a grayscale threshold for vugs. A constant was derived empirically by calibration with vuggy porosity values derived from digital images of slabbed-core samples and used to make the subtraction from the background baseline to derive the vug grayscale threshold as a function of azimuth. The method should be effective in estimating vuggy porosity in any carbonate aquifer.

Keywords: Digital borehole image log; Vuggy porosity; Borehole geophysics; Biscayne aquifer; Carbonates; Southeastern Florida

1. Introduction

Vuggy porosity is visible "pore space that is within grains or crystals or that is significantly larger than the grains or crystals; that is, pore space that is not interparticle" (Lucia, 1995). Intraparticle pores, particle molds, fenestrals, channels, vugs, and caverns of

* Corresponding author. Tel.: +1-305-717-5813; fax: +1-305-717-5801.
E-mail address: kcunning@usgs.gov (K.J. Cunningham).

0926-9851/$ - see front matter © 2003 Published by Elsevier B.V.
doi:10.1016/j.jappgeo.2003.06.006

Choquette and Pray (1970) are included in this definition. These kinds of porosity are all present in the Pleistocene limestone of the Biscayne aquifer and the larger well-connected type must play an important role in the flow of ground water through the aquifer. Although detection of vuggy porosity in the subsurface is a challenge, mapping the spatial distribution of vuggy porosity could produce significant insight into ground-water flow velocities and directions, salt-water intrusion, and movement of contaminants within carbonate aquifers.

Identification of vugs and fractures by geophysical logging is normally accomplished, in the absence of image logs, by combining and interpreting several logs, including: sonic, dipmeter, laterolog and induction, density, spontaneous potential, caliper, and natural gamma-ray spectrometry (Crary et al., 1987). A frustration to the environmental scientist is that identifications of vugs and fractures using these logs are challenging and interpretive in the absence of a borehole-wall image. We found that visual interpretations of digital borehole images are the most reliable and practical method of identifying vuggy porosity in the limestone of the Biscayne aquifer. With increased verification that electronic images of borehole walls in the quantification of vuggy porosity (Hickey, 1993; Newberry et al., 1996; Hurley et al., 1998, 1999) in petroleum reservoirs and fractures in aquifers (Williams and Johnson, 2000) can lead towards identification of

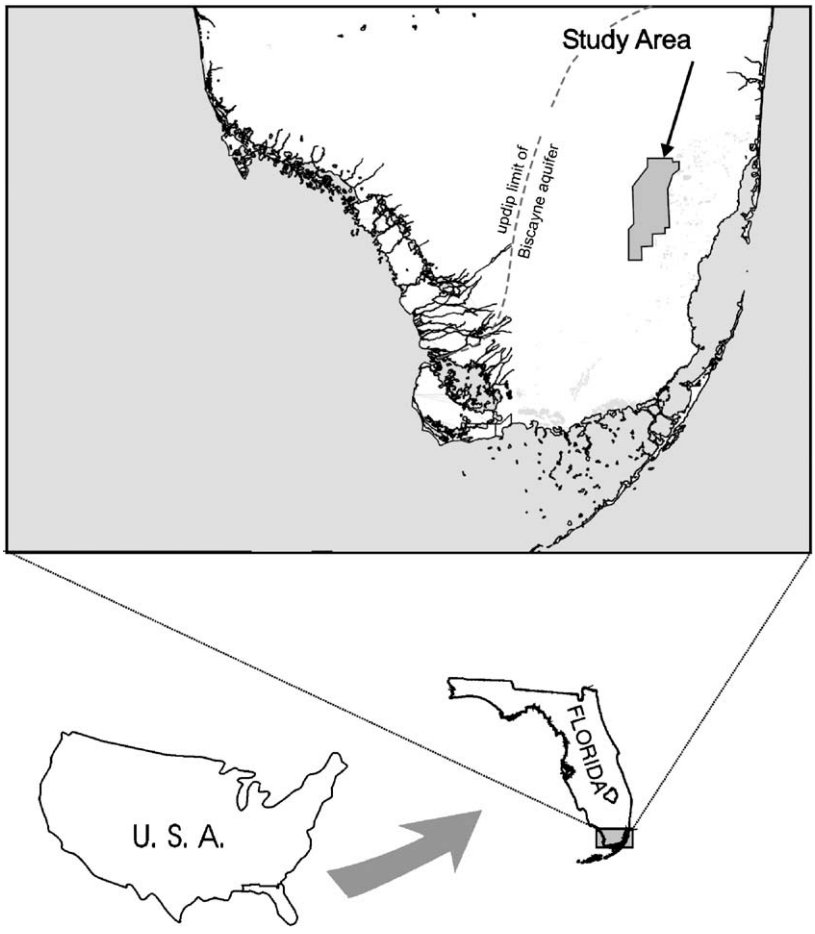

Fig. 1. Map of study area in north-central Miami-Dade County, southeastern Florida.

fluid-flow units, it was recognized that a method of quantifying digital borehole images collected in the limestone of the Biscayne aquifer needed to be developed.

The research methods presented in this paper are based on expansion of earlier work at the Institute for Resource and Environmental Geosciences at the Colorado School of Mines by Hurley and Alexander Aviantara. Carlson and Hurley developed the method of computing vuggy porosity and Carlson prepared the initial draft of the methods section. Cunningham described cores, supervised drilling of test coreholes, acquired the borehole-geophysical data, developed the high-resolution cycle stratigraphy, and participated in much of the final preparation of the manuscript and illustrations.

The purpose of this paper is to describe a new method of quantifying vuggy porosity in optical borehole images logged in coreholes drilled in the karstic Pleistocene limestone that comprises the Biscayne aquifer of southeastern Florida (Fig. 1). It is shown how an uneven illumination of the borehole wall due to eccentering of the image tool results in unbalanced digital grayscale images and how the method can be used to correct this problem to produce realistic values of vuggy porosity.

2. Drilling and borehole geophysical logs

The U.S. Geological Survey drilled 50 continuously cored test wells for this study using either a wireline coring system or conventional rotary coring system that collected whole-core samples. Geophysical logging was conducted on most of the test wells and included induction resistivity, natural gamma ray, spontaneous potential, single-point resistivity, caliper, and digital borehole image logs. The digital borehole image logs were run in 47 of the test wells while filled with clear fresh water using a RaaX™ Borehole Image Processing System (BIPS™) digital optical logging tool. RaaX™ designs BIPS™ for clear-water borehole environments to monitor, process, and record optical images of borehole walls in digital format for geological and geotechnical analysis. Upper and lower centralizers were used on the BIPS™ tool during logging of most test wells.

3. Stratigraphic nomenclature

The spatial distribution of vuggy porosity in the Pleistocene carbonate rocks of the Biscayne aquifer is controlled mostly by the distribution of deposi-

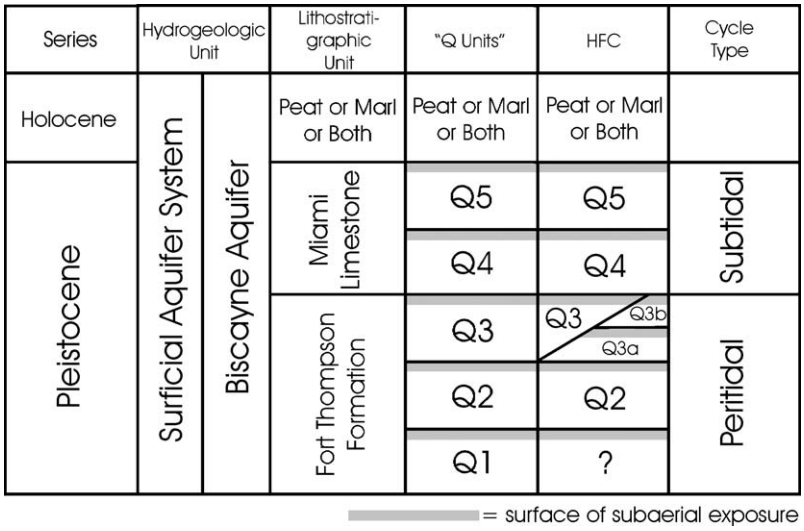

Fig. 2. Shallow time stratigraphic units, hydrostratigraphy (Fish and Stewart, 1991), lithostratigraphy (Causaras, 1987), "Q units of Perkins (1977), and high-frequency cycles (HFC) used in this paper for southeastern Florida.

tional textures, which is best described by a stratigraphic framework composed of high-frequency cycles (HFCs). Using a modified definition by Lucia (1999), the HFC is a chronostratigraphic unit composed of an unconformity-bounded succession of genetically related textures contained in beds or bedsets. The upper and lower bounding surfaces of the HFC are surfaces of subaerial exposure caused by a relative fall in sea level.

Two types of HFCs are present in the Biscayne aquifer. One is a subtidal cycle formed by vertical aggradation of high-energy shoals or shallow-marine, peloidal, highly burrowed sand flats. The Miami Limestone contains two unconformity bounded subtidal HFCs (Fig. 2). The second type of HFC, a peritidal cycle, is composed of a succession of depositional textures that decrease in grain size upward, that shallow upward, and is capped by a tidal-flat deposit or freshwater limestone or a stacking of both. Three peritidal HFCs are recognized in the upper part of the Fort Thompson Formation (Fig. 2). The delineation of HFCs in the lower part of the Fort Thompson is currently under investigation by the U.S. Geological Survey. The "Q" terminology of the HFCs is modified from Perkins (1977), who first recognized that the Miami Limestone and Fort Thompson Formation of south Florida are composed of five unconformity-bounded, time-stratigraphic marine units (Fig. 2). These units were informally termed, from oldest to youngest, Q1 through Q5 (Q for Quaternary). Fig. 2 shows the relation between the "Q units" of Perkins (1977) and the HFCs of this study.

4. Quantification of vuggy porosity

The development of a method for the quantification of vuggy porosity in borehole images of the limestone of the Biscayne aquifer required first the measurement of the proportion of vugs in images of slabbed whole-core samples, second the identification of vuggy porosity in borehole images, and finally, calibration of the core-sample values and results from borehole-images. The RECALL™ software manufactured by Baker Atlas™ provided the necessary tool to analyze and derive vug porosities in images.

4.1. Quantification of vuggy porosity from slabbed core

Twenty-five slabbed whole-core samples from 11 test coreholes were prepared for black and white photography by sanding the slab face to a smooth, flat surface. The slab face was then coated with a water-soluble printing ink using a soft rubber roller, which deposits the ink on the surface but does not penetrate into small vugs that are open at the slab surface. Two coats of ink were applied, a white nonfluorescent undercoat, then a topcoat of fluorescent orange ink that produces maximum photographic contrast between the rock and open vugs at the slab surface. The prepared slab surfaces were next photographed in a wooden exposure box while illuminated with fluorescent lighting. Hurley et al. (1998, 1999) describe in detail the core-sample preparation, and photographic equipment, film, and exposure settings used to obtain photographic results such as those shown in Fig. 3.

To obtain digitally scanned images of these core samples, photographic negatives of the "inked" slabbed-core surfaces were scanned using an Agfa

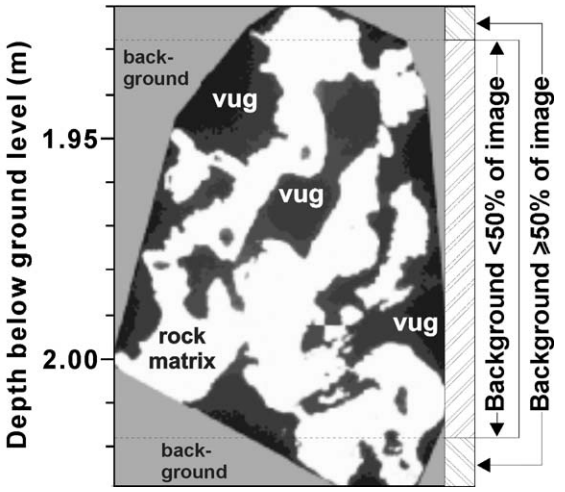

Fig. 3. Slabbed whole-core sample taken from the G-3725 test corehole in the depth interval between 1.92 and 2.03 m of the Q5 high-frequency cycle. Note the high porosity (dark gray to black) due to vugs. The rock is represented by white and surrounding background is the gray tone. Quantification of vuggy porosity was only conducted over that portion of the image where the proportion of the background was less than 50% of the sample image.

Duoscan™ flatbed scanner to produce a 230-level grayscale file of the negatives. Resulting grayscale images show the matrix as white and the vugs as dark gray to black (Fig. 3). The vug and rock-matrix image was trimmed in the software utility PHOTOSHOP™ to exclude any area outside of a polygon not defining the vug and rock-matrix image.

Images of core samples needed to be rectangular in order to facilitate processing. Fig. 3 shows the resulting core-sample image to which a background of medium-gray color has been added beyond the outside of the perimeter of the sample image (Fig. 3). Together, the background and the core-sample image form a rectangle that can be loaded into RECALL™.

RECALL™ provides an algorithm called STATISTICS™ that can analyze the proportion of vug, rock, and background according to their assigned color value at each available depth. This routine includes every available point in the scanned core image. The user provides the necessary precise thresholds: one between vug and background, and the other between background and rock matrix. Vug porosity is calculated as the proportion of the dark value divided by the sum of the dark and white portions. The results from STATISTICS™ can be plotted as a vug porosity curve beside the core image. To eliminate calculating vuggy porosities over areas that have small sample size and possibly nonrepresentative porosities, the following rule was applied using a user-defined software routine. If the gray background at each depth increment represented less than 50% of the image, then vuggy porosity was determined (Fig. 3). But, if the gray background was equal to or greater than 50% at each depth increment, vuggy porosity was not calculated. As an example, if the entire core-sample image in Fig. 3 was used, vug porosity would have been sampled from 1.92 to 2.03 m. However, the background rule reduces the interval from 1.928 to 2.018 m so that the available core interval is 0.02 m shorter (Fig. 3). For all 25 slabbed cores, approximately 92% of the available linear core depths were usable for vuggy porosity determination.

The results from STATISTICS™ can be plotted as a vug-porosity curve beside the core on a depth-by-depth basis (see column labeled COREPHI in Fig. 11) or presented as a single value that is the summation of all vug elements divided by all valid elements in the interval that defines the slabbed-core image (e.g., Fig. 3). The range of interval porosity values in Table 1 shows that the vuggy porosity values of the Q5 HFC span a much higher range than values for other HFCs. The very high porosity values contained in the Q5 HFC relative to underlying HFCs are consistent with whole-core laboratory measurement of porosity values presented by Cunningham (2003) for HFCs making up the Biscayne aquifer.

4.2. Identification of vuggy porosity in digital borehole images

Normally, defining grayscale thresholds that separate the vugs, rock matrix, and background portion of a digital image is a simple process of defining two grayscale-value cutoffs that bound the background values and applying STATISTICS™ as described in the paragraph above to calculate vuggy porosity. In the case of core-sample images, great care was taken to prevent uneven lighting of slabbed-core samples during sample photography, and the core samples were inked to create only two valid grayscale classes (dark gray to black and white) within the circumferential outline of core-sample images. However, in the case of the 47 digital borehole images, there are many valid values of grayscale that define vugs. A more critical problem is an uneven intensity of the light originating from the light source on the BIPS™ tool that illuminates the borehole wall. The differential intensity of borehole-wall illumination is due to tool eccentricity (whether centralizers were used or not), which defeats the capability of determining one grayscale cutoff that defines vug versus another that identifies rock matrix in the images. Fig. 4 shows an example of this problem, where there is a semivertical bright "stripe" along

Table 1
Interval vuggy porosity values for slabbed whole-core sample from high-frequency cycles

High-frequency cycle name	Number of cores	Range of interval vuggy porosity (%)
Q5	3	26.8–41.4
Q4	4	0.5–6.3
Q3b	3	0.01–10.4
Q3a	8	2.9–27.7
Q2 and Q1	7	0.3–7.3

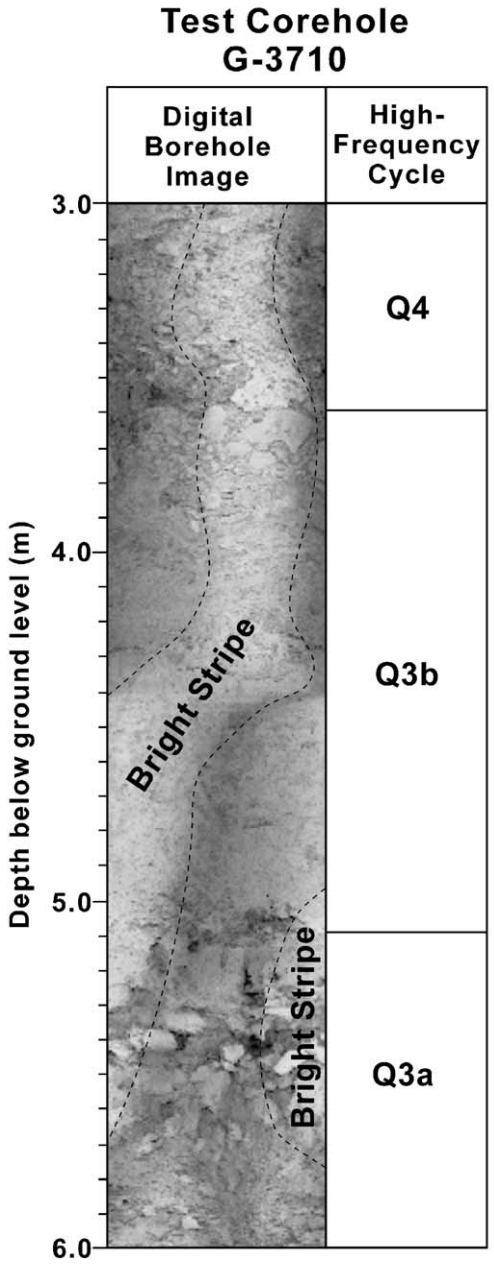

Fig. 4. Example of the digital borehole image. Note the longitudinal highlight effect that can be seen crossing the image. This effect is due to an eccentering of the image tool relative to the corehole circumference and tends to shift as the tool is moved up or down the corehole.

much of the borehole image due to eccentering of the tool. That portion of the borehole wall that is closer to the recording tool and light source appears brightest (Fig. 4). The eccentering of the borehole tool, and thus the light source, may change direction as the image of the borehole wall is recorded while the BIPS™ tool moves uphole or downhole. The uneven-lighting of the borehole wall produces an additional problem—a vug identified on the bright side of the borehole wall will have far greater contrast with the rock matrix than a similar vug in the darker side of the image. The human eye can identify both vugs and rock matrix, so an algorithm was necessarily designed to simulate this judgement.

Fig. 5 shows a model that demonstrates the lighting problem at a single borehole depth in a borehole image. In this representation of gray-scale values versus compass direction, it is assumed that the tool is eccentered and is closest to the borehole wall at 90° and farthest at 270°. The borehole surface is assumed to be completely smooth and homogeneous except for two vugs at 90° and 270°. An array of 670 elements represents all grayscale values sampled at this depth and encircling the borehole. Note the sine-like undulation of grayscale values that represents the effects of eccentered lighting with high grayscale values representing lighter grayscale tones than low values (Fig. 5). The vugs are identified as a lower value or darker grayscale tone than the neighboring background of the smooth and homogeneous borehole wall. Elements sampled at vugs on the bright side will have a greater value difference than those on the dark side (Fig. 5).

If the static STATISTICS™ technique, which was applied to core-sample images in RECALL™, was used on the depth shown in Fig. 5, both individual vugs could not be identified. For example, a threshold value of 115 for grayscale would identify the vug at 90°, but would also identify everything from 180° to 360° as a vug (Fig. 5). And, a threshold of 10 would only identify the vug found at 270° (Fig. 5).

Fig. 5 is an idealized representation of grayscale values that contrasts markedly with a much more complex graph of grayscale values at an actual depth from a digital borehole image shown by the solid-line curve in Fig. 6a. Fig. 6b shows an image of a 0.2-m-thick section of the borehole wall in test corehole G-3720. The grayscale values (670 elements sampled across the borehole-wall image) at the 5.0-m depth

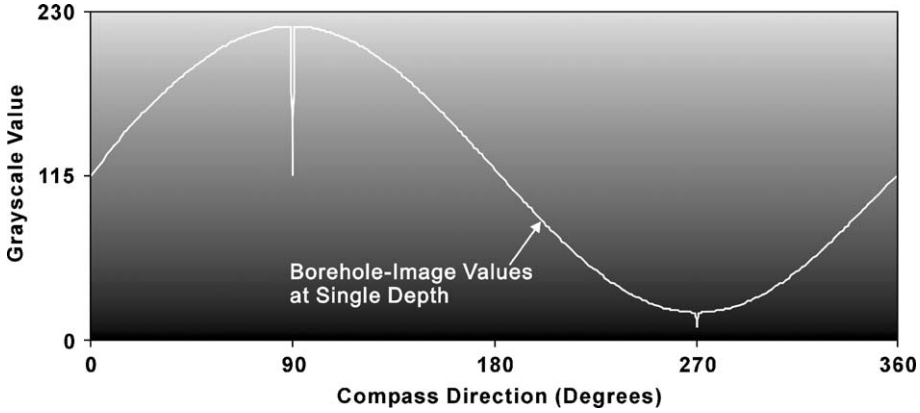

Fig. 5. Model of borehole-image grayscale values at a single depth of a digital borehole image. The sine-shaped curve shows the effects of eccentered lighting on the image and for two vugs (downward deflections of the curve). Note that the vertical distance between the peaks of the vugs and the sine-shaped background curve changes as the distance between the borehole and the tool changes.

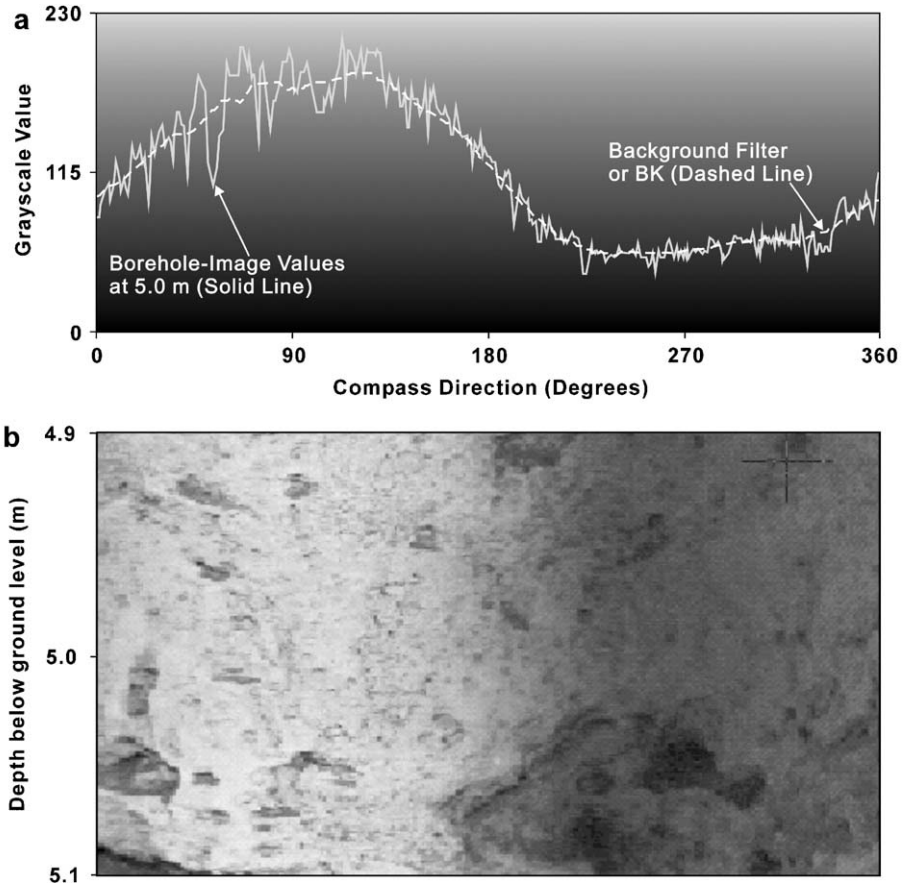

Fig. 6. Graph of the borehole-image grayscale values (solid line in (a)) at a depth of 5.0 m from the digital borehole image in (b). The background filter represented by the dashed line in (a) is called the BK curve, which is designed to remove the effects of eccentering. Any deflections of the solid line downward below the dashed BK curve are vuggy porosity candidates.

were retrieved and displayed as the solid-line curve in Fig. 6a. Vugs are represented by significant downward extensions of the solid-line curve that are more pronounced on the light side of the hole than the dark side. The grayscale curve (solid line) of the borehole-wall image in Fig. 6a is much more rugged than the smooth grayscale curve representing a model of the borehole-wall grayscale values shown in Fig. 5.

As shown in Fig. 6a, a moving-average curve (dashed line) called background (BK) was used to create a relatively smooth representation of the local variation of grayscale values along the circumference of the borehole wall. It was assumed that a moving average of the grayscale values spanning 1/8 of a borehole circumference was appropriate for normalization of BK for all borehole images. The borehole images were loaded into a matrix that was 670 elements wide, the 1/8 moving average used to approximate BK had a width of 84 elements. Local vugs represent a small percentage of the large average (84 elements) and did not, in general, affect the BK value. Even at a depth with many or large vugs, the moving-average curve represented the local change in light intensity along the borehole wall with candidate vug values appearing below the BK values (Fig. 6). The BK curve was calculated at every depth spanning an interval 2 mm in vertical height for each borehole image.

A method of counting potential vuggy porosity was devised by using the BK curve as a threshold and counting any grayscale value as a vug that falls below the BK curve. For instance, in Fig. 6, the total proportion of vuggy porosity at the depth of 5.0 m would be equal to the summation of counts for each element along the solid line that was below the dashed line divided by 670—the total possible counts. This background porosity (BGED) calculated at each depth is an important key to calibrating vug core porosity to the digital borehole images. A display of the results of this technique is shown in track 3 of Fig. 7. Comparison of the borehole image in track 1 and the image in track 3 indicates that the black areas representing

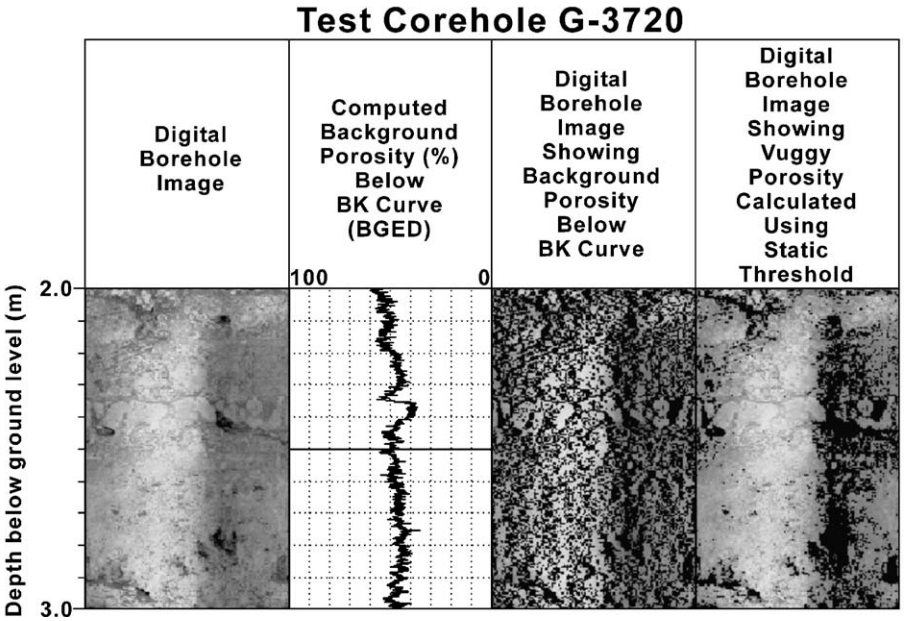

Fig. 7. Digital borehole image, computed porosity, and digital borehole images with blackened porosity from two depth intervals in test corehole G-3720. The first track shows the original digital borehole image from 2- to 3-m depth below ground level. The third track shows what the image would look like if every grayscale color below the background or BK were considered a vug. The results shown in track 3 are recorded as background porosity in track 2 and has a range of 38–60%. Track 4 shows the portion that would be considered vugs (black) in the same image if the effects of eccentering were ignored and a static grayscale threshold was used. Note the predominance of vug incorrectly identified on the dark side of the image in track 4 while the brightest portion is almost totally devoid of vugs.

potential vugs are evenly spaced but too abundant to be considered valid vugs (Fig. 7). But, most importantly, the most poorly illuminated (darker) side of the borehole wall does not show an increased number or extent of vugs, and is not totally black, as is almost the case in track 4 where a static or single grayscale threshold provided by the STATISTIC™ algorithm was utilized. So, the attempt to neutralize the effects of uneven lighting of the borehole wall was successful and the final task was to calibrate this moving-average technique for vug computation.

Recalling that vug contrast is greater in the brighter side of the hole, the next step was to design a threshold that is below the 84-element moving average (BK) and is thicker in the bright zones and thinner in the dark zones, as shown by the thickness between the dashed and solid lines in Fig. 8. Vugs are identified as all values that fall below the dashed-line or threshold curve (Fig. 8). A percentage of the grayscale value, *P*, below the BK curve provides the threshold, but it requires calibration with core-sample images. Eq. (1) expresses a preliminary threshold curve.

$$\text{Threshold} = (1 - P)\text{BK} \tag{1}$$

where BK is the moving-average curve derived from 670-grayscale-image values along the circumference of the borehole-wall image at a single depth, and *P* is a constant that provides a vuggy-porosity threshold expressed as a fractional percentage.

Vuggy porosity is calculated as the summation of elements at a given depth that are less than the vuggy-porosity threshold (Fig. 8) divided by the number of elements evaluated (670 elements), as expressed in Eq. (2).

$$\text{Image Vuggy Porosity} = \text{vc}/\text{ct} \tag{2}$$

where vc is the count of the number of grayscale values below vuggy-porosity threshold at a single depth, and ct is the number of elements (670) evaluated around the borehole wall at a single depth.

After a reasonable value for *P*, the constant in Eq. (1), was established by calibration of vug porosity of the core to the digital image, vug porosity for every depth in the 47 digital borehole images could be calculated.

4.3. Calibration of vuggy porosity in digital borehole images and slabbed-core images

Deriving vuggy porosity on a depth-by-depth basis in all the digital borehole images was achieved by calibrating the vuggy porosity determined in the core-sample images with observations of the digital-borehole-image and modeled-borehole-image data. The concepts and data used to do this included: (1) a reliable calculation of vuggy porosity for the 25 core-sample images at 2-mm depth increments, (2) a model that eliminates the effects of eccentering, (3) the calculation

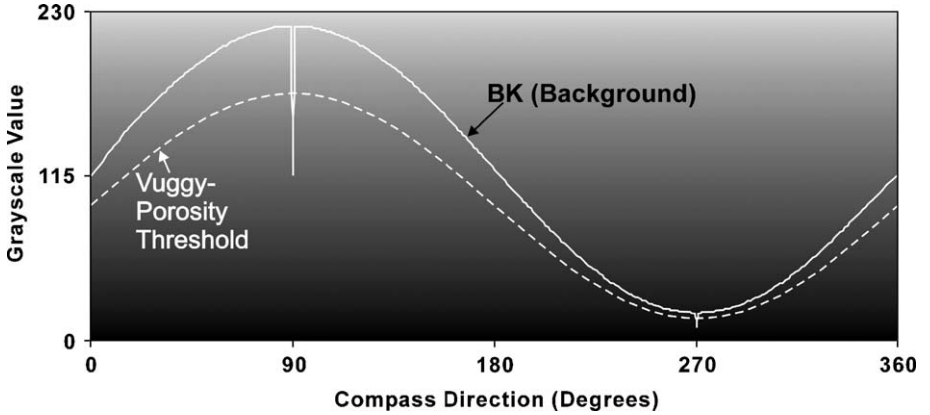

Fig. 8. A model of the data presented in Fig. 5 with the addition of a dashed line representing the threshold or cutoff (see Eq. (1)) that will identify all vugs around the borehole and eliminate the problems of an eccentered tool. All data that falls below the threshold is counted as vuggy porosity.

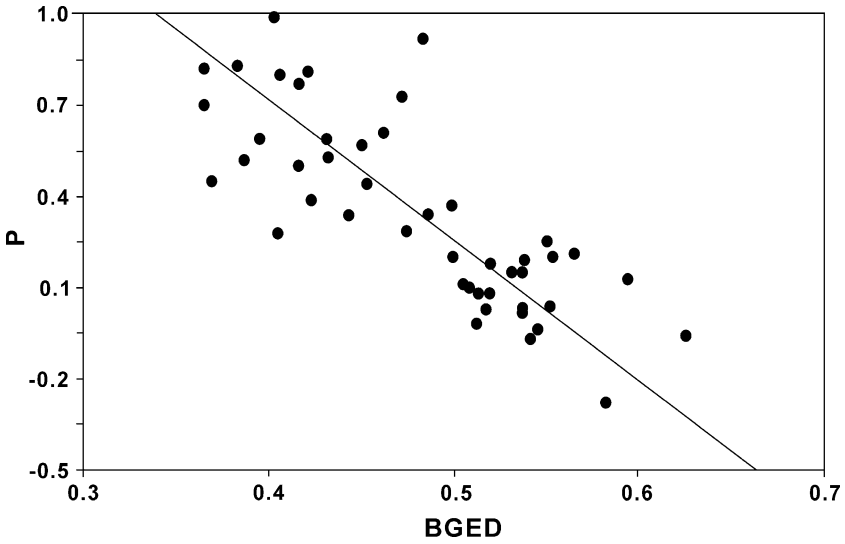

Fig. 9. Scatter plot of the background porosity or BGED versus the best value of *P* that will produce the same vuggy porosity in the borehole images as that found in the 25 core samples. This relationship produces the necessary value of *P* for Eq. (1).

of BK curves through moving averages at 2-mm depth increments in the 47 digital borehole images, and (4) an estimate of background porosity (BGED) at every depth using the BK curve as a vuggy porosity threshold (method described earlier to produce track 2 in Fig. 7, or Eq. (2), where *P* is zero in Eq. (1)).

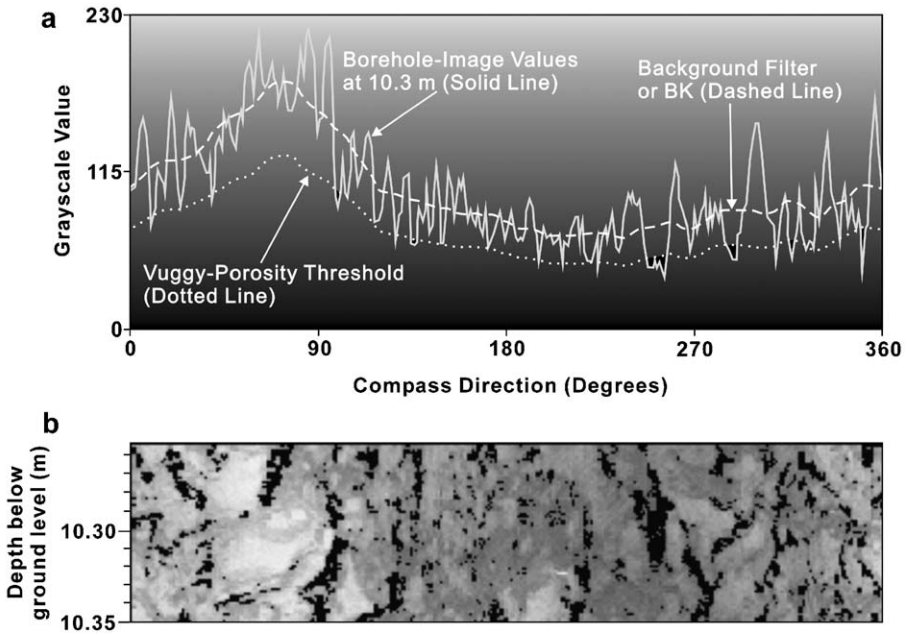

Fig. 10. (a) Graph shows the grayscale values from the depth 10.3 m (solid line) and the background curve BK (upper dashed line). Any points that fall below the vuggy-porosity threshold curve (lower dotted line) are considered vuggy porosity. (b) Digital borehole image used to generate data presented in (a).

After the calculation of the vuggy porosity in the 25 core-sample images, the next step was to establish a relationship between the vuggy porosity derived from core-sample images and the data at the same depth intervals as the digital borehole images. A vuggy porosity value calculated from an image was not expected to exactly match the vug porosity from slabbed-core images. This is because the borehole image is a circumferential view of the rock comprising a borehole wall, while the slabbed-core image is a view of a planar cross section of a cylinder of rock that has been inked and was present in the interior of the borehole wall. It is assumed that the vug porosity derived from the slabbed-core images is highly accurate on a depth-by-depth basis. Even if slabbed-core images are correctly matched to depths of borehole-wall images, it is not expected that a peak-to-peak or trough-to-trough match between curves of vuggy porosity values of core and borehole images would exist. However, overall shapes and magnitudes of curves should be similar, as shown by comparing tracks 2 and 3 in Fig. 11. Keys (1986) presents a similar sample mismatch with comparison of porosity measured on core plotted against neutron-log values, and Paillet and Crowder (1996) discusses in detail how samplings of two different

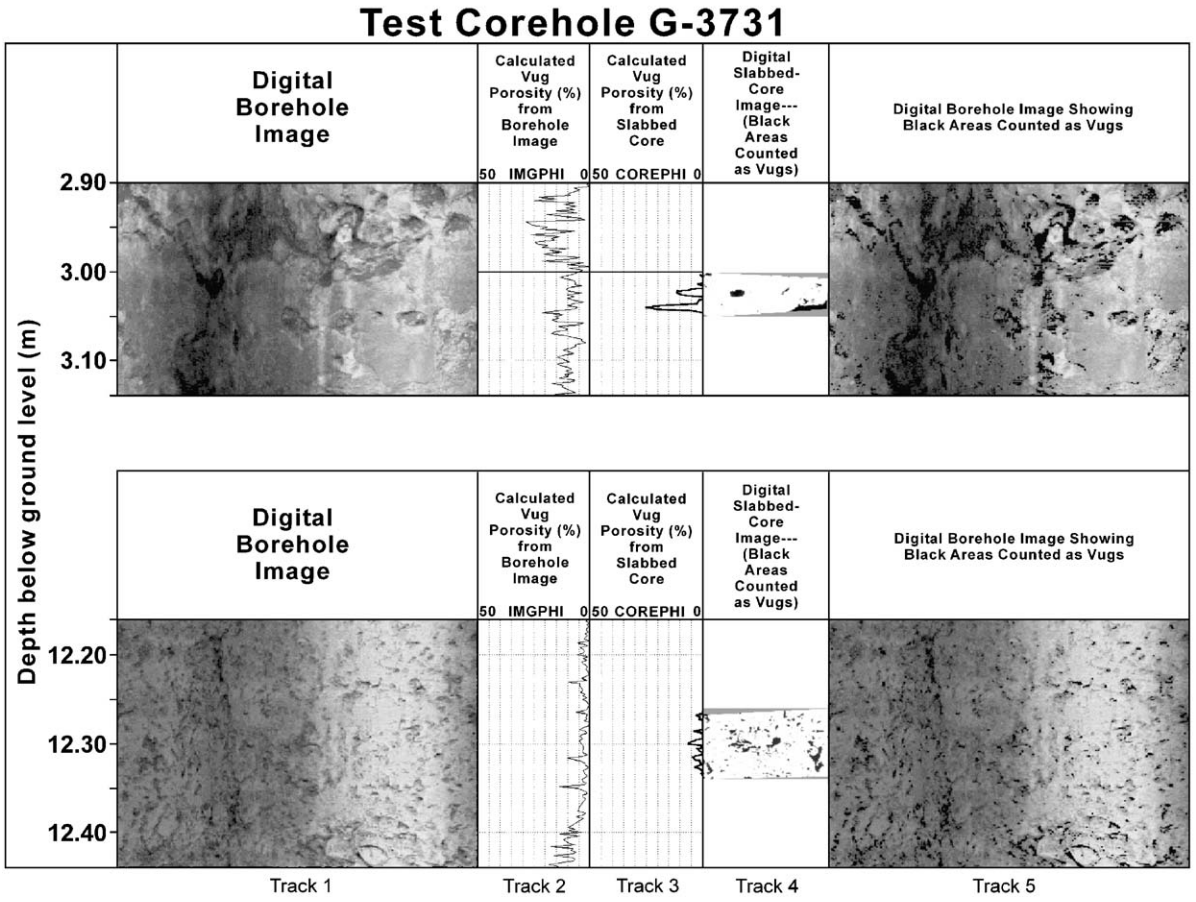

Fig. 11. Plots of two depth intervals in G-3731 showing the comparison of core to digital image and the resulting calculations of vug porosity on a depth by depth basis. Track 1 contains the original digital image. Track 5 on the far right contains the same image with the portions determined to be vugs darkened. Tracks 2 and 3 contain the vug porosity determined from the image (IMGPHI) and the vug porosity determined from the slabbed core (COREPHI). Track 4 shows the photographed slabbed core where white is rock matrix, black is vug contribution, and the gray surrounding the core is background (where no analysis can be made).

parameters at the same depth can result in different vertical distributions of log attributes.

To establish the relation between core and borehole image, it was assumed that the highest vuggy porosity value for any row of elements in a core-sample needs to match the highest BGED (an estimate of background porosity) for any row of elements in the same interval of the borehole image. An iterative test was then applied using Eqs. (1) and (2) to establish a best P that would provide the same highest vuggy-porosity value from borehole-image data as highest core-image value. The same method was applied to the minimums in each core. This exercise provided 50 points for Fig. 9 that established a relationship between BGED and P based on minimum and maximum porosities from the core-sample images.

A scatter plot of the data, BGED and P, assumes a linear relationship with a high negative correlation coefficient of -0.8 (Fig. 9). A regression line that minimizes the average of the sum of squares error in the x and y directions applied to the data predicts a value of P from BGED in Eq. (3).

$$P = 2.56764 - 4.62344 \times \mathrm{BGED} \quad (3)$$

where P is the necessary constant needed to calibrate the background curve in Eq. (1) to produce the threshold for vug determination, and BGED is the porosity using the BK curve as a threshold at a single depth.

Fig. 10 is an example of applying P to a BK curve at a single depth (10.3 m) to produce a vuggy-porosity threshold. Elements along the 10.3-m depth are counted as vuggy porosity where the solid-line curve representing the borehole-image values is below the vuggy-porosity threshold (lower dashed line in Fig. 10).

4.4. Testing of quantification of vuggy porosity in digital borehole images

Testing of this technique was, by examination of the calculated vuggy porosity curve in the core-

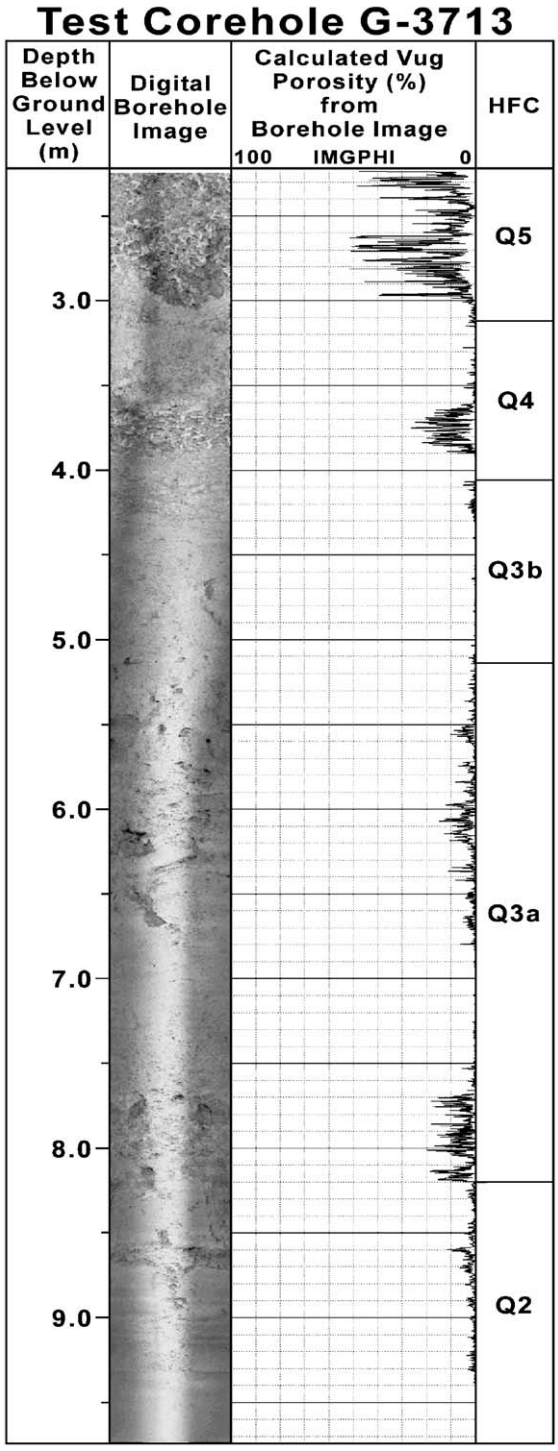

Fig. 12. An example of a vuggy porosity log display of limestone from a portion of the Biscayne aquifer showing the original digital borehole image, the calculated vug porosity (IMGPHI) from the image, and the high-frequency cycles (HFCs).

sample intervals and comparison of it to the vuggy porosity curve, calculated for the corresponding borehole image. A second test was to compare the digital borehole image with the predicted vugs darkened to the core image for visual inspection. Fig. 11 shows two core-sample images from test corehole G-3731 where the resulting estimate of vuggy porosity from the borehole image (marked IMGPHI) and the vuggy porosity from the core image (marked COREPHI) is an excellent match. Visual inspection of the size and density of vugs also look similar in the core-sample image of track 4 and the darkened areas of the digital borehole image in track 5. All 25 core-sample images were compared to the vuggy porosity predicted from the digital borehole images by reviewing the darkened borehole image and comparing the vuggy porosity curves. Approximately 90% of the predicted values looked reasonable.

5. Conclusions

A new method has been developed for quantifying vuggy porosity in digital borehole images that emphasizes removing the effects of an eccentralized image tool and extracting the darkest values from the images as vugs. It is observed that the vugs were not consistently dark in the original images and this method will not identify them, making the predicted vug porosity a conservative estimate. However, 90% of the depths yielded conservative vug porosity values that were reasonable in value and image presentation. The method should be effective in estimating vuggy porosity in any carbonate aquifer.

Fig. 12 shows a sample of the final graphical representation of vuggy porosity determined for one of the 47 borehole images processed in the southeastern Florida study area (Fig. 1). As shown in Table 1, porosity values are exceptionally high in the Q5 HFC, as noted by Cunningham (2003) for laboratory porosity measurement of whole-core samples from many of the same coreholes used herein. High porosity values were found to be common at the base of the Q3a HFC and are related to the vertical stacking of lithofacies within the Q3a HFC. This observation is consistent with data presented by Cunningham (2003) that shows the lower portions of HFCs contained within the upper Fort Thompson Formation have statistically significant lower total porosity values than middle and upper portions of the HFCs.

Acknowledgements

This project was funded in part by the South Florida Water Management District. Jean-Claude Poix, Anthony Brown, and Marc Buursink assisted with field activities. The Branch of Geophysics, USGS, provided essential geophysical instrumentation and technical advice during field activities. Fred Paillet and James LoCoco are thanked for critical reviews.

Note: The use of brand names in this paper is for identification purposes only and does not constitute endorsement by the authors, the U.S. Geological Survey, or the Journal of Geophysics.

References

Causaras, C.R., 1987. Geology of the surficial aquifer system, Dade County, Florida. U.S. Geol. Surv. Water Resour. Invest. Report 86–4126.

Choquette, P.W., Pray, L.C., 1970. Geologic nomenclature and classification of porosity in sedimentary carbonates. Am. Assoc. Pet. Geol. Bull. 54, 207–250.

Crary, S., Dennis, R., Denoo, S., et al., 1987. Fracture detection with logs. Tech. Rev. 35, 22–34.

Cunningham, K.J., 2003. Application of ground-penetrating radar, digital optical borehole images, and cores for characterization of porosity and paleokarst in the Biscayne aquifer, southeastern Florida. J. Appl. Geophys. 55, 61–76 (this volume).

Fish, J.E., Stewart, M., 1991. Hydrogeology of the surficial aquifer system, Dade County, Florida. U.S. Geol. Surv. Water Resour. Invest. Report 90–4108.

Hickey, J.J., 1993. Characterizing secondary porosity of carbonate rocks using borehole video data [abstract]. Abstr. Programs-Geol. Soc. Am. 25, p. 23 (Southeastern Section).

Hurley, N.F., Zimmermann, R.A., Pantoga, D., 1998. Quantification of vuggy porosity in a dolomite reservoir from borehole images and core, Dagger Draw Field, New Mexico. Soc. Petrol. Engineers 49323, Annual Technical Conference and Exhibition, New Orleans, Louisiana, September 27–30, 1998, pp. 789–802.

Hurley, N.F., Pantoja, D., Zimmerman, R.A., 1999. Flow unit determination in a vuggy dolomite reservoir, Dagger Draw Field, New Mexico. SPWLA Transactions, 4 Oslo, Norway. 14 pp.

Keys, W.S., 1986. Analysis of geophysical logs of water wells with a microcomputer. Ground Water 24, 750–760.

Lucia, F.J., 1995. Rock-fabric/petrophysical classification of carbonate pore space for reservoir characterization. Am. Assoc. Pet. Geol. Bull. 79, 1275–1300.

Lucia, F.J., 1999. Carbonate Reservoir Characterization. Springer-Verlag, Berlin.

Newberry, B.M., Grace, L.M., Stief, D.D., 1996. Analysis of carbonate dual porosity systems from borehole electrical images. Soc. Petrol. Engineers (SPE) Paper 35158, Permian Basin Oil and Gas Recovery Conference, Midland, TX, 123–125.

Paillet, F.L., Crowder, R.E., 1996. A generalized approach for the interpretation of geophysical well logs in ground water studies: theory and application. Ground Water 34, 883–898.

Perkins, R.D., 1977. Depositional framework of Pleistocene rocks in south Florida. In: Enos, P., Perkins, R.D. (Eds.), Quaternary Sedimentation in South Florida, Part II. Geol. Soc. Am. Mem. 147, 131–198.

Williams, J.H., Johnson, C.D., 2000. Borehole-wall imaging with acoustic and optical televiewers for fractured-bedrock aquifer investigations. Proceed. Minerals and Geotech. Logging Symp., Golden, CO, October 24–26, pp. 43–53.